Generation of a subpicosecond relativistic electron single bunch at the S-band linear accelerator

Mitsuru Uesaka, Kenichiro Tauchi, Takahiro Kozawa, Toshiaki Kobayashi, Toru Ueda, and Kenzo Miya
Nuclear Engineering Research Laboratory, University of Tokyo, 2-22 Shirakata-Shirane, Tokai-mura, Naka-gun, Ibaraki 319-11, Japan
(Received 2 June 1994)

A subpicosecond 37-MeV electron single bunch was generated at the *S*-band linear accelerator of the University of Tokyo. An original single bunch with a pulse width [full width at half maximum (FWHM)] of less than 10 ps was successfully compressed to a subpicosecond time domain by magnetic pulse compression. Here the energy profile of electrons in a bunch is modulated in the longitudinal direction by tuning the phase of a traveling microwave in an accelerating tube. The electrons in the earlier and later halves in the bunch have higher and lower energy, respectively. Then, the above energy modulation is transferred to a path length modulation by a magnetic optics system formed by a dipole and a quadrupole magnet assembly to achieve pulse compression, in other words, bunch compression. The energy modulation was optimally matched to the magnetic optics to achieve the most effective compression by tuning the rf power and the phase of the microwave. A femtosecond streak camera with a time resolution of 600 fs was utilized to measure a pulse shape of electron bunches by one shot via Cherenkov radiation emitted by the electrons in xenon or air. The specification of optical components was also optimized to avoid pulse broadening due to optical dispersion. Finally, the shortest and average pulse widths in FWHM are 0.7 and 0.9 ps in the best operating mode, respectively. The compressed bunches have an electric charge of 0.15 nC (9.4×10^8 electrons) in average. Prior to the experiment, numerical tracking analysis for electrons in the pulse compressor was performed to investigate the matching between the energy modulation and the magnetic optics. Experimental and numerical results with respect to pulse widths were compared with each other and discussed. Space charge effects on longitudinal pulse lengthening were also analyzed using relativistic electrodynamics. The subpicosecond electron single bunch is going to be utilized for exploration of ultrafast and fundamental radiation physics and chemistry.

PACS number(s): 41.75.−i

I. INTRODUCTION

Femtosecond technology [1] is going to become a key technology to investigate ultrafast and fundamental quantum beam induced phenomena. So far the Ti-sapphire laser has been the only radiation source to generate ultrashort laser light pulse in a femtosecond time domain [2,3]. Ultrafast phenomena such as excitation, ionization, and relaxation of atoms and molecules have been investigated using a femtosecond laser and an ultrafast measurement system [4,5]. On the other hand, from the viewpoints of radiation physics, chemistry, and material science, the exploration of ultrafast and fundamental phenomena induced by high energy particle beams in a femtosecond time domain has been expected to have great importance. Those phenomena can be measured via light emission and absorption [6,7]. Especially the dynamics of atomic cascade damage induced by particle beams is expected to be analyzed via accompanying light emission. Up to now, only numerical molecular dynamics is a tool for this research [8]. Thus the development of a femtosecond particle beam source and light measurement system can contribute not only to beam technology but also to femtosecond physics, chemistry, and technology. A relativistic electron beam generated by a radio frequency (rf) linear accelerator is the most promising candidate for the purpose.

A 10-ps [full width at half maximum (FWHM)] electron single bunch was first generated at the 35 MeV *S*-band linear accelerator (linac) with the subharmonic buncher and the pulse radiolysis system was established in 1977 [9,10]. Since then the system has been contributing to the research of ultra fast and basic processes of radiation chemistry in picosecond and nanosecond time domains by measuring light emission or absorption of matter irradiated by the 10-ps electron bunch. In particular the twin linac and stroboscopic absorption measurement system were built in 1986 [11]. Here the bunch generated by the first time irradiates a specimen and the Cherenkov radiation pulse emitted in air by the bunch generated by the second linac is used as a probe light. The twin linac system has enabled the absorption measurement in a picosecond time domain. On the other hand, a 9-ps single bunch with 20 nC was generated at the *L*-band linac of Osaka University in 1986 [12] and a 5-ps single bunch with 4 nC was generated at the *L*-band linac of Argonne National Laboratory in 1986 [13]. In those cases the original bunches were compressed by the magnetic pulse compression technique. Very recently the 10-ps electron single bunch was compressed to 2 ps by using a preliminary magnetic compressor at the linac of University of Tokyo [14]. As to relativistic electron multibunches, the *L*-band injector linac supplies electron multibunches with a pulse width of less than 2 ps to the 4-GeV superconducting continuous-wave ring-shaped linac at the Continuous Electron Beam Accelerator Facil-

ity [15]. Wiedemann, Kung, and Lihn have constructed a linear accelerator with a rf electron gun to produce ultrashort electron multibunches and photon pulses in a femtosecond time domain [16]. Concerning electron multibunches and synchrotron radiation, several investigations on bunch length controlling have been reported [17], but the pulse width is limited up to about 100 ps due to the low frequency rf cavity used in a synchrotron or storage ring. Considering the above progress and achievement, we have entered the stage seeking a new system to investigate super-ultra-faster phenomena of beam-matter interaction in a femtosecond time domain. For this purpose a femtosecond electron single bunch is necessary. The research on magnetic pulse compression aiming at generating a femtosecond single bunch began recently at the linac of University of Tokyo. The main objective of this paper is to report and discuss how to generate and measure a femtosecond electron single bunch with a certain amount of electric charge at the *S*-band linac. A numerical tracking analysis was also done to determine the operating parameter for the magnetic pulse compression experiment.

II. EXPERIMENTAL SETUP

The *S*-band twin linac is schematically depicted in Fig. 1. The twin linac consists of the two linacs named 28L and 18L. The maximum energy is 38 MeV. 28L has two accelerating tubes (ACC1, ACC2) into which rf power is fed by a klystron (KLY1). 18L has an accelerating tube (ACC3) into which rf power is fed by another klystron (KLY2). The experiments were performed at 28L. The bunch structures and energy spectra of the original single bunches riding on different rf phases in ACC1 and ACC2 were precisely investigated and their longitudinal phase space distributions were evaluated previously [14]. The magnetic pulse compression experiment was carried out at 28L. The magnetic pulse compressor consists of the two accelerating tubes (ACC1 and ACC2), a bending magnet, which is normally used as an energy analyzer magnet, two quadrupole magnets, and another bending magnet as shown in Fig. 2. Those components have just been assembled and the specification is not necessarily optimized. ACC1 and ACC2 were used for acceleration and energy modulation, respectively. A single bunch is

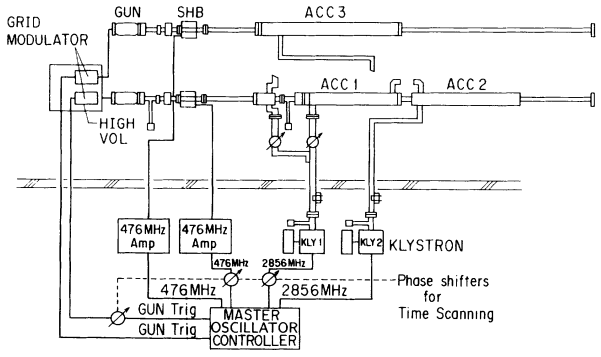

FIG. 1. *S*-band electron twin linear accelerator of the University of Tokyo.

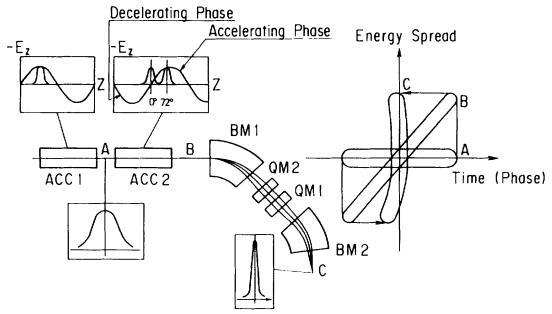

FIG. 2. Schematic drawing of a magnetic pulse compressor and the transformation of a longitudinal phase space distribution. The time or phase stands for the longitudinal coordinate so that the early electrons lie in the right region. The bunches riding on the 0° and 72° rf phases in ACC2 represent the cases of the linear and nonlinear energy modulations.

accelerated up to 19.1 MeV in ACC1 and the rf phase in ACC2 is tuned in such a way that it rides on a specified rf phase of the traveling accelerating field wave. This tune-up yields the energy modulation of the electrons where the electrons in the early and later halves of the bunch have higher and lower energy, respectively. The two bunches riding on the 0° and 72° rf phases in ACC2 in the figure represent the cases of linear and nonlinear energy modulations, respectively, as discussed later. Then, this energy modulation is converted to a pulse length modulation by the magnet assembly so that the pulse compression, namely, the bunch compression in the longitudinal direction, is achieved. The variation of the longitudinal phase space of the compressed bunch is also schematically depicted in the figure. In the longitudinal phase space, the horizontal and vertical axes represent relative time difference and energy spread with respect to the center of the bunch. The time or phase at the horizontal axis stands for the longitudinal coordinate so that the early electrons lie in the right region. The connection of the waveguides between the accelerating tubes and klystrons was made so that the klystrons can feed the rf power independently into ACC1 and ACC2 with tunable phase shift. The energy modulation, which is determined by the nonlinear slope of the accelerating electric field, is controlled by varying the rf power and phase in ACC2. The slope is automatically determined from the peak electric field and rf phase since the traveling electric field can be approximated to be sinusoidal. Hereafter we use the peak electric field and rf phase as an indicator of the energy modulation. The calibration between the rf power and the peak accelerating field was performed by the following measurement beforehand. Once the rf power was fixed, the maximum energy gain of a single bunch was investigated by varying the rf phase and the average peak accelerating field was evaluated from the measured maximum energy gain.

Pulse shapes were obtained by measuring Cherenkov radiation by one shot emitted by the electrons of a bunch in xenon or air at the end of the 45° bent beam line, namely, the compressor. The experiment was performed twice at different machine times. At first, the bunches

ride on the zero-cross rf phase so that the energy modulation is almost linear with respect to the longitudinal coordinate. Since the mean energy of the bunch accelerated by only ACC1 is limited up to 19.1 MeV, which is less than the threshold energy ($E_{th}=20$ MeV) for Cherenkov radiation in air (1 atm; refraction index $n=1.000\,29$), we attached a xenon gas ($E_{th}=12$ MeV at 1 atm; refraction index $n=1000\,78$) chamber at the end of the 45° bent beam line to generate Cherenkov radiation. At the second experiment the single bunches ride on the rf phase from 45° through 72° so that the best matching between the energy modulation and magnetic optics is obtained for best pulse compression. In this case the mean beam energy is far higher than 20 MeV and the electrons can emit Cherenkov radiation in air and the xenon chamber was removed for convenience of the optical measurement then. The optical measurement system to guide the Cherenkov radiation to the streak camera is shown is Fig. 3. We used three mirrors, a convex lens, and an optical filter. Its optical pass is almost 3 m long. In particular we utilized a femtosecond streak camera which has a time resolution of 600 fs (HAMAMATSU FESCA-500, by courtesy of the Free Electron Laser Institute, INC, Japan). We chose a slit width of less than 30 μm in order to avoid the pulse broadening due to space charge effects in the camera. Furthermore, an optical band pass filter, which is centered at 465 nm and has a half width of 12.5 nm, was used to avoid the pulse broadening due to optical dispersion in the convex lenses used in the measurement. This measurement with extremely high time resolution is available by using the sophisticated trigger system of our linac [18]. Especially, the trigger pulses synchronized by a specified rf phase can be generated and used to trigger the electron gun and the streak camera. The jitter of this measurement is less than 10 ps, which is speculated to come from the trigger jitter at the streak camera so far. All data of compressed pulse shapes were acquired by single shot measurements. On the other hand, the energy spectra were obtained in a conventional manner using the energy analyzer magnet. The beam sizes in the horizontal and vertical directions in FWHM were evaluated by using a phosphor screen monitor and image processing system. The electric charge per bunch was measured by using the Faraday cage, which is represented as a beam catcher in Fig. 3.

III. ELECTRON TRACKING ANALYSIS

To find the peak electric field in ACC2 and the field gradient in the quadrupole magnets for most effective pulse compression, the numerical electron tracking analysis was carried out beforehand. An electron in a single bunch can be tracked in the first-order approximation with help of the well-known transformation analysis [19] in the following. The coordinate system is depicted in Fig. 4. The equation of motion of an electron in the horizontal direction is written as

$$m\frac{d^2r}{dt^2}=m\frac{v^2}{r}-evB\ , \tag{1}$$

where m is the relativistic mass, r is the coordinate of the electron position in the x direction, v is the velocity, e is the electric charge of an electron, and B is the vertical dipole magnetic field for example. Suppose that the perturbation of the transverse coordinate (x or y) is very small compared to the Larmor radius in the bending magnetic field. We linearize and generalize Eq. (1), considering a quadrupole magnet, a drift space, and the motion in the x and y directions, as

$$u''+K(s)u=\frac{1}{\rho}\delta\ , \tag{2}$$

where u stands for x or y, and $K(s)$ is a constant which depends on magnetic field configurations such as a dipole or quadrupole magnet or a drift space, and the prime represents the derivation with respect to s. If we assume the magnetic field to be homogeneous in the longitudinal direction in a cell such as dipole and quadrupole magnets and a drift space, Eq. (2) is applied to get the following linear relation between the x and y coordinates and the momentum perturbation of the electron at the entrance and exit of the cell:

$$\begin{bmatrix} u(s_{out}) \\ u'(s_{out}) \\ \delta \end{bmatrix}=\mathbf{T}\begin{bmatrix} U(s_{in}) \\ u'(s_{in}) \\ \delta \end{bmatrix}\ , \tag{3}$$

where s_{in} and s_{out} are the longitudinal coordinates of the entrance and exit of the cell and $\mathbf{T}$ is the transformation matrix. By Eq. (3) the position of the electron at the en-

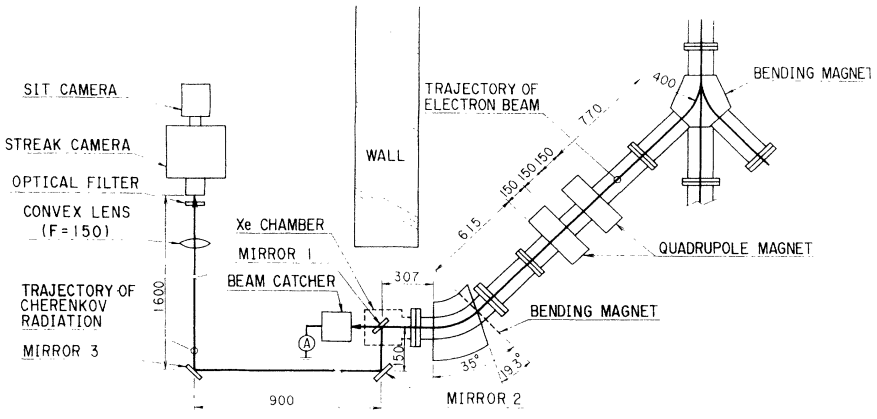

FIG. 3. Magnetic pulse compressor and Cherenkov radiation measurement system.

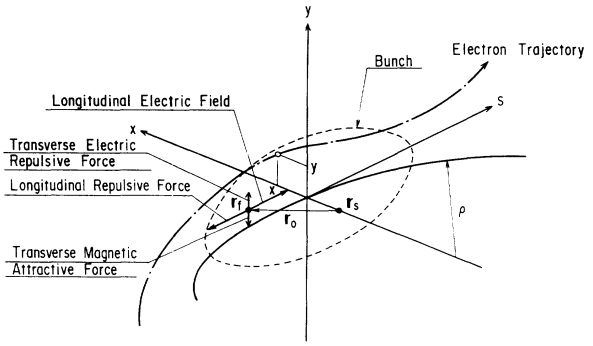

FIG. 4. Coordinate system in the tracking analysis and space charge effect calculation (○, electron for the tracking analysis; ●, particle for the space charge effect calculation).

trance and exit of cells can be calculated. Once the position of the electron is calculated at the entrance and exit of each cell, the length of the trajectory in the cell can be determined. Since the speed of the electron can be assumed to be the speed of light, the time or phase shift can be evaluated. The position of the electron is shifted in the horizontal direction in the longitudinal phase space because its energy is conserved. Thus the longitudinal phase space distribution is obtained at the exit of each cell and finally at the first mirror in the optical measurement system as shown in Fig. 3. The magnetic pulse compression in the preliminary compressor was analyzed by this transformation matrix method and the calculated pulse width of 4 ps was about twice as long as the measured value of 2 ps [14].

The above transformation matrix method is based on the perturbation theory where all quadratic or higher-order terms are neglected. Actually, an error of 0.3 mm in the path length of an electron corresponds to a 1-ps time difference, which is unacceptable for the discussion of pulse compression in a subpicosecond time domain. For a more rigorous discussion we have numerically tracked electrons in a bunch passing through the pulse compressor by solving the following three-dimensional equation of motion:

$$\frac{d(m\mathbf{v})}{dt} = e\mathbf{v}\times\mathbf{B} \ . \tag{4}$$

We assumed that the magnetic fields in the dipole and quadrupole magnets are assumed to be homogeneous in the longitudinal direction. The path of an electron in a homogeneous vertical magnetic field can be analytically calculated with the transverse position and velocity at the entrance of the dipole magnet so that the position and velocity vector at the exit can be obtained. As for the quadrupole magnet, we divided it into 100 longitudinal subdomains where an electron experiences constant vertical field. Under the above assumption the path of the electron in each subdomain can be calculated in the same manner as for the dipole magnet. Thus the path in the whole quadrupole magnet is evaluated. The longitudinal phase space distribution at the exit of each cell is constructed by the same procedure as that used in the transformation matrix method. The field leakage from the yoke of the magnets was measured and the correction for it was done by adjusting the field strength. This task is referred to as the direct tracking method.

TABLE I. Beam parameters used in the numerical tracking analysis.

Initial energy accelerated by ACC1	19.1 MeV
Beam profile	Gaussian
Pulse width (FWHM)	9 ps
Energy spread (FWHM)	0.2%
Horizontal and vertical emittance (90% normalized)	100π nm mrad
Peak accelerating Electric Field in ACC2	0–9.3 MV/m

Beam parameters used in the analysis are summarized in Table I. All values are previously measured ones. The initial distributions of electrons in the horizontal, vertical, and longitudinal phase spaces at the entrance of ACC2 are assumed to be Gaussian with standard deviations obtained from the values in Table I. The shape of the distributions in the horizontal and vertical phase spaces is assumed to be circular for simplicity. 1000 electrons are generated according to the Gaussian distributions and their positions in the phase spaces are calculated at the end of each cell by making use of both the direct tracking method and the transformation matrix method. The pulse width and the energy spread are evaluated as the FWHMs of the density distributions of the electrons in the horizontal and vertical directions in the longitudinal phase space, respectively. First we consider

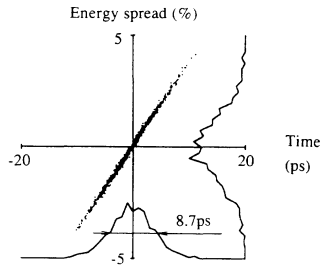

(a) At the exit of ACC2

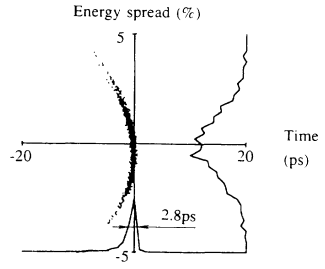

(b) At the first mirror

FIG. 5. Calculated longitudinal phase space distribution in the linear energy modulation mode by the direct tracking method.

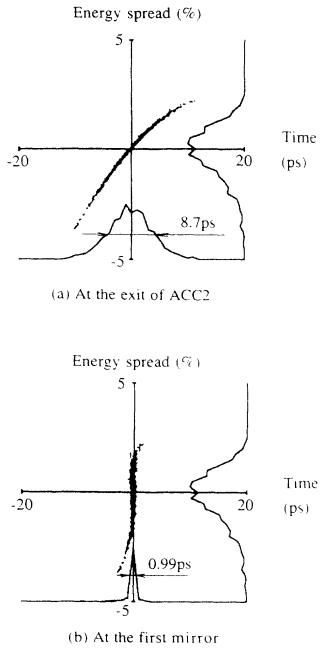

FIG. 6. Calculated longitudinal phase space distribution in the nonlinear energy modulation mode by the direct tracking method.

the case that the bunch rides on the zero-cross rf phase in ACC2 and the peak longitudinal electric field is 2.0 MV/m. Hereafter we call this case the linear energy modulation mode, since the linear slope in the vicinity of the 0° phase is utilized. The calculated phase space distribution of the 1000 electrons in the bunch at the exit of ACC2 and at the first mirror by the direct tracking method is shown in Fig. 5. Although the pulse compression from 8.7 to 2.8 ps is achieved, the shape of the distribution is rather distorted. This can be attributed to the nonlinearity of trajectory modulation, namely, phase shift in the phase space, to momentum perturbation, namely, energy spread. The pulse compression efficiency is limited due to this effect. This effect can be compensated by the nonlinear slope near the crest of the sinusoidal electric field. The calculated phase space distribution at the exit of ACC2 and at the first mirror is shown in Fig. 6, where the bunch is supposed to ride on the 72° phase of the rf wave with a peak field of 9.3 MV/m. It is clear that the shape becomes more straight and parallel to the vertical axis. The analysis tells us the prospect that a subpicosecond single bunch might be generated at this linac.

Another issue which has to be considered here is the pulse elongation due to space charge effects in the bunch. To analyze this effect, we use the following relativistic electromagnetic fields at a field point $\mathbf{r}_f$ generated by an electron at a source point $\mathbf{r}_s$ (see Fig. 4):

$$\mathbf{E}=-\frac{q}{4\pi\varepsilon_0}\left[1-\left[\frac{\mathbf{v}}{c}\right]^2\right]\frac{\mathbf{r}_0}{s^3}\,,$$
$$\mathbf{B}=\frac{\mu_0 q}{4\pi}\left[1-\left[\frac{\mathbf{v}}{c}\right]^2\right]\frac{\mathbf{v}\times\mathbf{r}_0}{s^3}\,, \tag{5}$$

where

$$\mathbf{r}_s=(x_s,y_s,z_s)\,,$$
$$\mathbf{r}_f=(x_f,y_f,z_f)\,,$$
$$\mathbf{r}_0=\mathbf{r}_f-\mathbf{r}_s\,,$$
$$s=\left[|\mathbf{r}_0|^2-\left[\frac{v}{c}\right]^2[(y_f-y_s)^2+(z_f-z_s)^2]\right]^{1/2}.$$

Terms of radiation due to the acceleration of the source electron are neglected because of the relatively low electron energy. Because the Coulomb repulsion is almost balanced with the magnetic attraction in the transverse direction in the relativistic energy region, we consider and calculate only the longitudinal Coulomb repulsion. In the calculation, a set of particles, which are assumed to be a cluster of an equal number of electrons, is generated in a single bunch according to the Gaussian distribution in both the transverse and longitudinal directions.

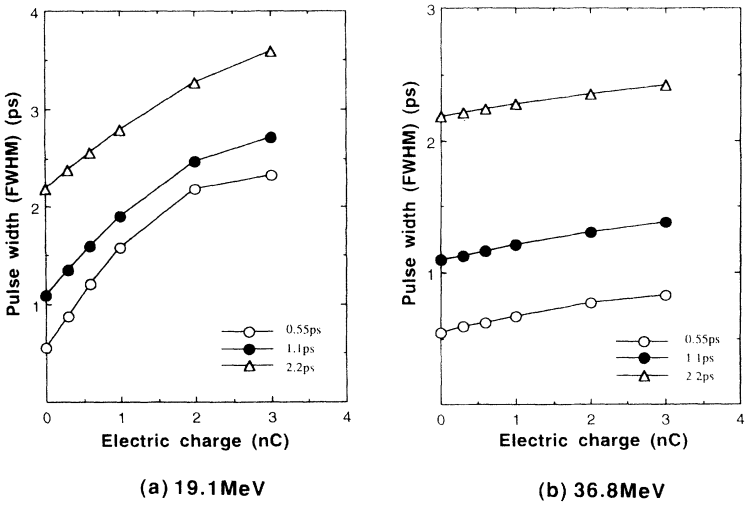

FIG. 7. Calculated longitudinal pulse elongation due to the space charge effect.

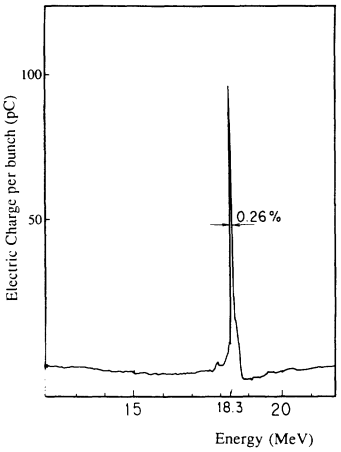

FIG. 8. Energy spectrum of a single bunch accelerated by ACC1.

The number of particles is fixed to be just 300 since the capability of our computer (Sun-microsystems-ELC) is limited. The longitudinal Coulomb repulsive force acting on each particle by other particles is calculated and the equation of motion involving the force is solved and the pulse elongation is evaluated as a variation of the FWHM of the longitudinal distribution of the particles in the bunch. The variation of the pulse width of a bunch with a mean energy of 19.1 and 36.8 MeV with the electric charge of the bunch through a 0.5-m-long drift space is shown in Fig. 7. Initial pulse widths of 0.55, 1.1, and 2.2 ps are considered here. It is observed that the pulse elongation is weaker as the mean energy increases due to the Lorentz contraction. Since the electric charge per bunch is limited up to 1 nC in the linac, the space charge effect is negligible for a picosecond or subpicosecond single bunch of around 36.8 MeV.

IV. RESULTS AND DISCUSSION

A. Linear energy modulation

In the magnetic pulse compression experiment, the rf phase in ACC1 was tuned so as to make a single bunch ride almost on the crest. The energy spectrum of the bunch was measured as shown in Fig. 8. Its energy spread in FWHM is 0.26%, which coincides with the value used in the tracking analysis (see Table I). As mentioned in previous sections, we utilized the linear slope of the rf in ACC2 in the first experiment. The rf phase in ACC2 was tuned so as to accelerate electrons in

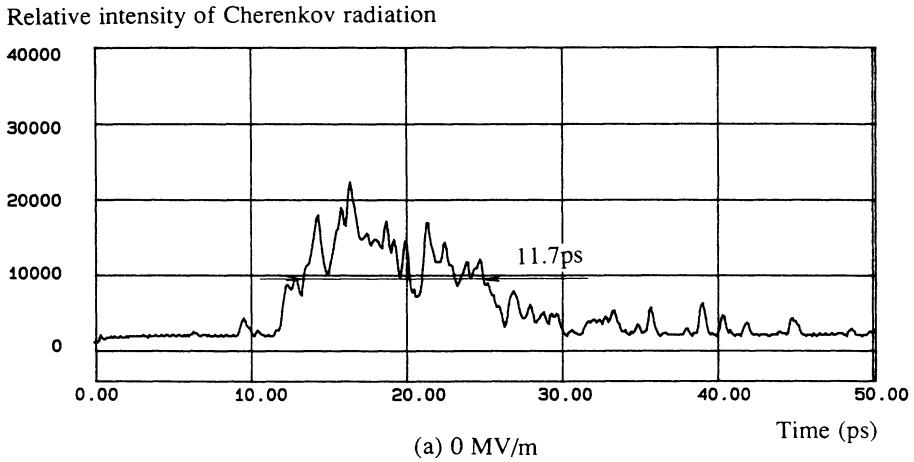

(a) 0 MV/m

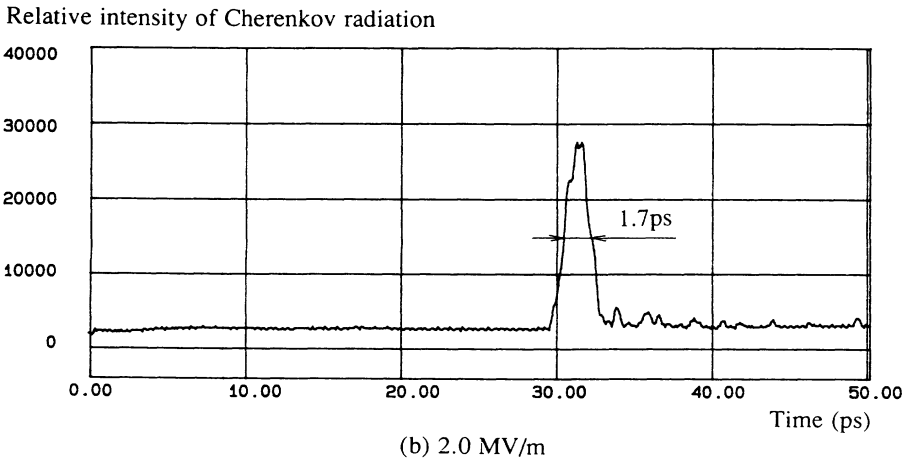

(b) 2.0 MV/m

FIG. 9. Measured pulse shapes of 19.1-MeV original and compressed single bunches for the peak electric fields of 0 and 2.0-MV/m in ACC2.

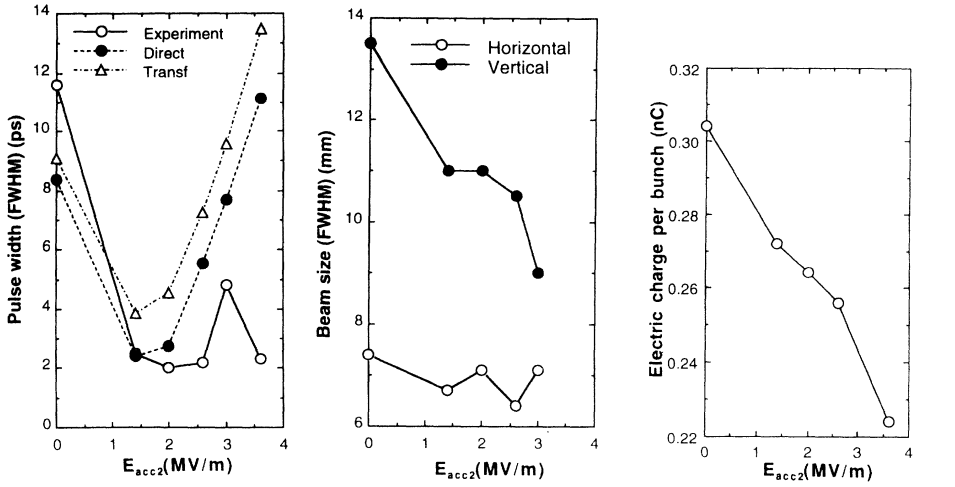

FIG. 10. Pulse width, beam size, and electric charge per bunch as a function of the peak electric field in ACC2 for the linear energy modulation.

the early half of the bunch and to decelerate those in the alter half. We varied the peak electric field in ACC2 in order to control the energy modulation and measured the pulse width with a single shot. Typical measured pulse shapes for 0 and 2.0 MV/m in ACC2 are shown in Fig. 9. In the case of 2.0 MV/m the averaged pulse width among ten compressed bunches is 2.0 ps. Measured pulse widths, x- and y-beam sizes in FWHM, and electric charge per bunch are plotted as a function of the peak electric field, namely, the energy modulation, as shown in Fig. 10. Since the measurement was done ten times for each case, the circles stand for the averaged values. Since

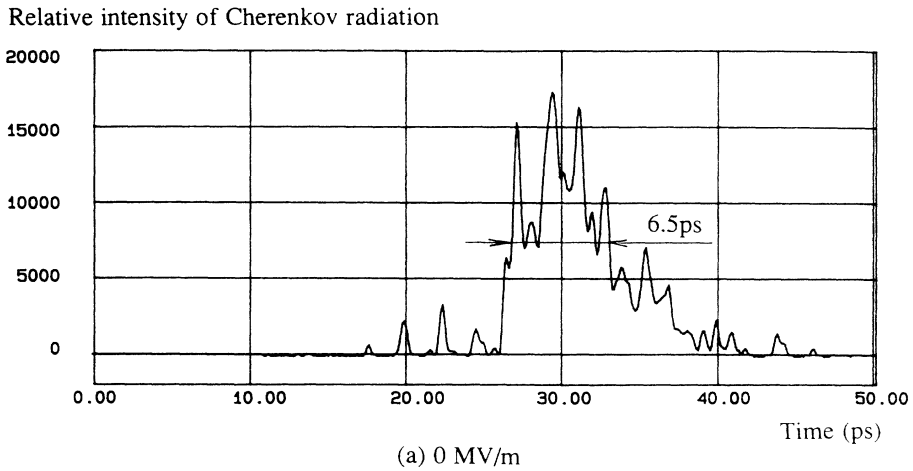

(a) 0 MV/m

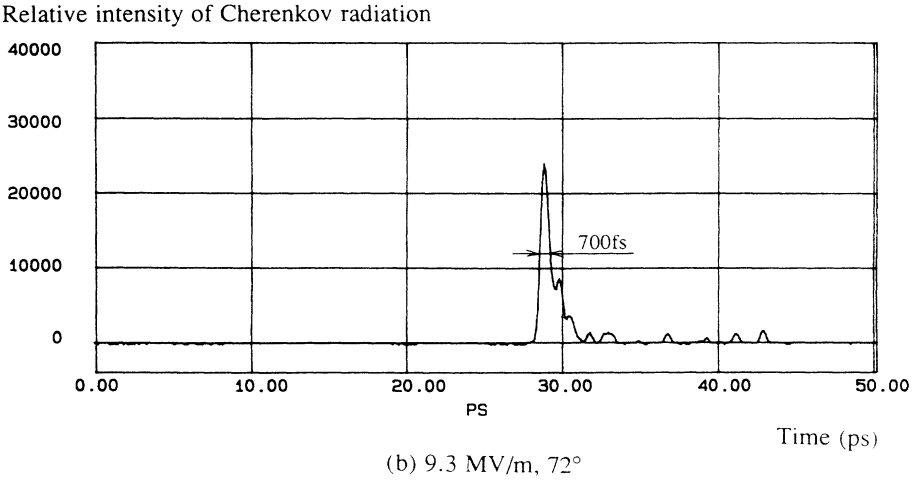

(b) 9.3 MV/m, 72°

FIG. 11. Measured pulse shapes of 36.8-MeV original and compressed single bunch riding on the rf phase of 72° for the peak electric fields of 9.3 MV/m in ACC2.

the pulse compressor does not form an achromatic optics, the beam sizes in both the horizontal and vertical directions are rather large. Calculated pulse widths by the transformation matrix and direct tracking methods without the space charge effect are compared with each other and with the measurement as shown in the figure. The deviation of the transformation matrix method from the direct tracking method is about 2 ps. The shorter pulse and few electric charges for more than 2 MV/m in the experiment can be attributed to the loss of electrons at the inner wall of the vacuum chamber and Ti window and the resultant poor signal-to-noise ratio because the bunch is rather spread in the horizontal direction due to its rather strong energy modulation. It can be said that the latter results fairly agree with the experimental results. This comparison validates the computer codes without the space charge effect for the magnetic pulse compression of a single bunch containing less than 1 nC in a picosecond or subpicosecond time domain. Finally, it can be concluded that a 2.0-ps single bunch of 0.26 nC could be generated by the linear energy modulation. An achromatic pulse compressor is planned to be installed in order to achieve much higher luminosity in near future.

B. Nonlinear energy modulation

If the energy modulation is linear to the longitudinal coordinate or phase or time, the final phase space distribution is rather distorted and the pulse compression efficiency is limited due to the nonlinearity of the trajectory modulation to the energy modulation as shown in Fig. 5. In order to compensate this effect and enhance the efficiency, we make use of the nonlinear slope of the sinusoidal rf wave in ACC2 as predicted by the tracking analysis as shown in Fig. 6. The peak electric field in ACC2 was fixed to be 9.3 MV/m, which corresponds to the maximum rf input and the rf phase was scanned by the phase shifter. The operation of the pulse compressor was tuned according to the variation of the mean energy of the bunches riding on the different phase in ACC2. Typical measured pulse shapes of 36.8 MeV original single bunch and compressed single bunch riding on the phase of 72° are shown in Fig. 11. It is found that the 6.5-ps pulse width of the original single bunch was shorter than the 10 ps of the 19.1-MeV original single bunch. This could be ascribed to the bunching during the acceleration from 19.1 to 36.8 MeV in ACC2. The best matching between the nonlinear energy modulation and trajectory modulation and the above shorter initial pulse width yielded the compressed single bunch of the pulse width of 0.7 ps. The average pulse width among 10 shots was 0.9 ps. Based on the careful investigation of measurement error, we have so far concluded that the time resolution of this measurement is limited by the bandwidth of the optical filter, which is used to eliminate the optical dispersion. For better time resolution, we plan to use the optical filters with a bandwidth of less than 10 nm. Measured pulse width, beam sizes, and electric charge per bunch are summarized in Fig. 12. Pulse widths calculated by the direct tracking method are included in the figure. Again good agreement between the experiment and calculation was achieved. The reason why the calculated pulse width is shorter than the measured one for the phase of 45° also can be ascribed to the loss of electrons at the inner wall of the vacuum chamber due to large horizontal beam spread. Finally, the subpicosecond single bunches with the electric charge of 0.15 nC, where the shortest and average were 0.7 and 0.9 ps, respectively, were generated for the rf phase of 72° and the peak electric field of 9.3 MV/m in ACC2.

Although the 36.8-MeV subpicosecond electron single bunch was obtained, its electric charge was limited up to 0.15 nC and its beam sizes were rather large. Especially the reason for the few electric charges is under consideration. We plan to construct an achromatic magnetic pulse compressor to overcome the above problems and supply subpicosecond electron single bunches of high luminosity

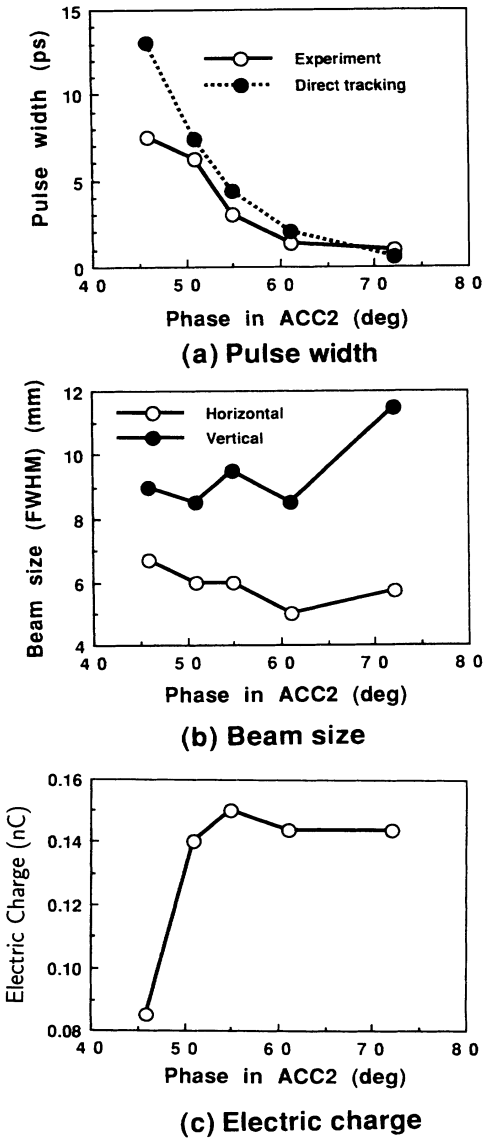

FIG. 12. Pulse width, beam size, and electric charge per bunch as a function of the rf phase in ACC2 for the nonlinear energy modulation.

to radiation physics and chemistry research in the near future.

Here we demonstrated the possibility of generating a subpicosecond electron single bunch at the *S*-band linear accelerator. As a future step we have to consider what we should do if a femtosecond single bunch with a pulse width of less than 100 fs is needed. It is clear from Figs. 6 and 9 that a high compression efficiency such as 11–14 % was achieved and that the energy spread and emittance of the original bunch also looked dominant to the pulse width of the compressed bunch. Considering our experience of the recent compression experiments with the 10-ps original bunches, the compressed bunch looks to be close to the shortest limit at the *S*-band linear accelerator. On the other hand, we may be able to generate a femtosecond single bunch of about 100 fs if we use a short original bunch such as a few picoseconds and its energy spread and emittance are much improved. For the former purpose we may have to choose and *X*-band (11.424 GHz) accelerating system, which is now under development for linear colliders. We also have to develop an electron gun and a buncher system with a higher emittance and quality for the latter purpose. After we construct the achromatic magnetic compressor, we are to proceed to consider the above two challenging issues.

V. SUMMARY

A subpicosecond 37-MeV electron single bunch was generated at the *S*-band linear accelerator of University of Tokyo. An original single bunch with a pulse width of less than 10 ps (FWHM) was successfully compressed to a femtosecond time domain by magnetic pulse compression with nonlinear energy modulation. The energy modulation was optimally matched to the magnetic optics to achieve the most effective compression by tuning the rf power and phase of the accelerating microwave. The femtosecond streak camera with a time resolution of 600 fs was utilized to measure the pulse shape of electron bunches from single shot Cherenkov radiation emitted by the electrons in xenon or air. The specification of optical components was also optimized to avoid the pulse broadening due to optical dispersion. Finally, the shortest and average pulse widths in FWHM ar 0.7 and 0.9 ps in the best operating mode, respectively. The compressed bunches contain an electric charge of 0.15 nC (9.4×10^8 electrons) on average. Numerical tracking analysis using the transformation matrix and direct tracking methods was performed and the results were compared with each other and the experiment. Finally, the error of the former was evaluated and the latter was adopted to investigate the matching between the energy modulation and magnetic optics. The space charge effect on the longitudinal pulse elongation was found to be negligible for high energy of about 37 MeV and a total bunch charge of less than 1 nC. A more efficient magnetic pulse compressor is planned to be constructed and the subpicosecond electron single bunch of high luminosity is going to be utilized for exploration of ultrafast and fundamental radiation physics and chemistry in the near future.

ACKNOWLEDGMENTS

The authors would like to thank Dr. Takio Tomimasu and other researchers of the Free Electron Laser Institue, INC for their collaboration on the measurement using the fermtosecond streak camera and Professor Atsushi Ogata of National Laboratory of High Energy Physics for his collaboration on the pulse compression experiment.

[1] *Proceedings of the International Workshop on Femtosecond Technology (FST'94), Tukuba, Japan, 1994* (New Energy and Industrial Technology Development Organization of Japan, (Tukuba, 1994).
[2] A. Migus *et al.*, IEEE J. Quantum Electron. **18**, 101 (1982).
[3] J. G. Fujimoto, A. M. Weiner, and E. P. Ippen, Appl. Phys. Lett. **44**, 832 (1984).
[4] C. K. Sun *et al.*, Phys. Rev. B **48**, 12 365 (1983).
[5] S. B. Fleischer *et al.*, Appl. Phys. Lett. **62**, 3241 (1993).
[6] C. D. Jonah, Rev. Sci. Instrum. **46**, 62 (1975).
[7] Y. Tabata, Radiat. Phys. Chem. **18**, 43 (1981).
[8] K. Morishita, N. Sekimura, and S. Ishino, J. Nucl. Mater. **191-194**, 1123 (1992).
[9] Y. Tabata, J. Fac. Eng. Univ. Tokyo **34B**, 619 (1978).
[10] Y. Yoshida *et al.*, Radiat. Phys. Chem. **30**, 83 (1987).
[12] M. Kawanishi *et al.*, Mem. Inst. Sci. Ind. Res., Osaka Univ. **43**, 3 (1986).
[13] G. L. Cox *et al.*, Proc. of the 1989 Particle Accel. Conf., CONF-890335–271 (unpublished).
[14] M. Uesaka *et al.*, Nucl. Instrum. Methods Phys. Res. A **345**, 219 (1994).
[15] W. Barry, P. Kloeppel, R. Rossmanith, Los Alamos National Laboratory, Report No. LA-12004-C, 719 (990), (unpublished).
[16] H. Wiedemann, P. Kung, and H. C. Lihn, Nucl. Instrum. Methods Phys. Res. Sect. A **319**, 1 (1992).
[17] H. Hama, S. Takano, and G. Isoyama, Nucl. Instrum. Methods Phys. Res. Sect. A **329**, 29 (1993).
[18] H. Kobayashi *et al.*, Nucl. Instrum. Methods **179**, 223 (1981).
[19] H. Wiedemann, *Particle Accelarator Physics* (Springer, Berlin, 1993).